60-13

EUROPEAN ORGANIZATION FOR NUCLEAR RESEARCH

PAPER FOR THE EEC

31 January, 1966

AN EXPERIMENTAL PROPOSAL
TO MEASURE THE PRODUCTION OF (e^+e^-) PAIRS FROM TIME-LIKE PHOTONS
PRODUCED IN PION-NUCLEON INTERACTIONS

P. Dalpiaz, G. Fortunato,
T. Massam, Th. Muller and A. Zichichi.

66/197/3

1. INTRODUCTION

The process which we wish to study is the production of (e^+e^-) pairs in pion-nucleon interactions, i.e.

$$\pi + N \rightarrow e^+ + e^- + N.$$

The corresponding Feynman diagram is:

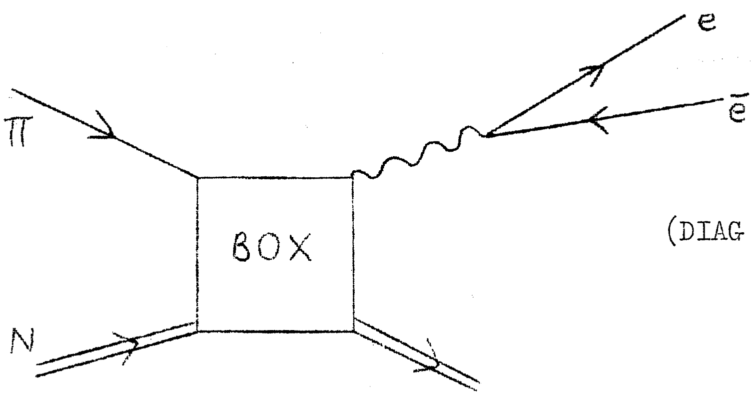

(DIAG A)

Such an investigation has many interesting aspects which we will try to summarize in the following paragraphs.

i) If the dispersion integrals of the nucleon form factors contain important contributions from a non-resonant background, this will show up directly in our experiment by the fact that e^+e^- pairs will also be observed at q^2 values other than those at the ρ, w and φ peaks. As is well known, "pole dominance" is extremely appealing because of its simplicity, and consequently people involved in this field prefer to maintain this working hypothesis until there is evidence to the contrary.

The best fit obtained by Massam and Zichichi shows that the non-resonant background can be maintained as low as 5%. It is obvious that the observation of a large non-resonant background, which could also be q^2 dependent, would be of tremendous importance for what would turn out to be our present misunderstanding of nucleon form factors.

In the following we will limit ourselves to the case of "pole dominance" in order to show that if "pole dominance" turns out to be true, then very interesting problems in our present-day physics can be investigated.

ii) If the dispersion integrals of the nucleon form factors are dominated by poles, then the structure of the box in DIAG A is the following:

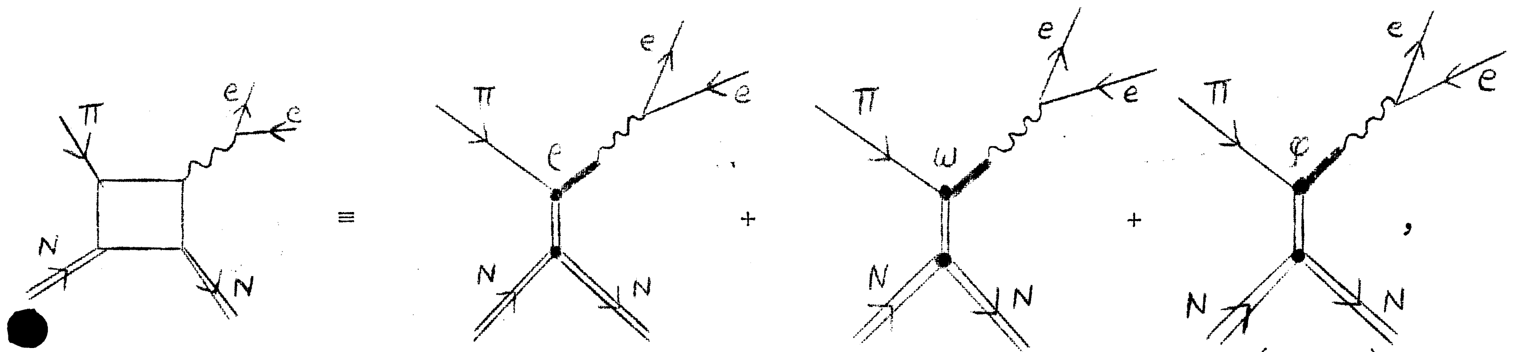

(DIAG B)

that is, the production of (e^+e^-) pairs with high time-like q^2 values will proceed essentially via those intermediate states which are the known vector meson resonances: ρ, ω, φ.

66/197/3
p/jmf

This will allow us to check that the known vector mesons (ρ, ω, φ) play the role which we think they play in the electromagnetic structure of the nucleons. As this point has been fully discussed by one of us in a recent CERN seminar, we will not illustrate this point further.

iii) The measurement of the (ω-φ) mixing angle. The physical particles ω and φ are believed to be mixtures of a pure SU_3 singlet ω_0 and a pure 8^{th} member of an SU_3 octet ω_8, i.e.

$$\varphi = \omega_8 \cos \Theta_s + \omega_0 \sin \Theta_s$$

$$\omega = - \omega_8 \sin \Theta_s + \omega_0 \cos \Theta_s .$$

The angle Θ_s determined from the mass formula is

$$\Theta_s = 38^\circ \pm 2^\circ .$$

(This cannot in fact be considered as a measurement of Θ_s, but is rather a way of adjusting the mass formula.)

An independent way of determining Θ_s has been suggested by Sakurai, namely that of comparing the experimental width of $\varphi \to \bar{K} + K$, $\Gamma_{\varphi \to K\bar{K}}$, with the one predicted from the knowledge of Γ_ρ and Γ_{K^*}; the two widths are in fact related:

$$\Gamma_{\varphi \to K\bar{K}} = \cos^2 \Theta_s \cdot \Gamma_{\omega_8 \to K\bar{K}} ,$$

since the unitary singlet ω_0 cannot contribute to the channel $K\bar{K}$. In fact, ω_0 can only be coupled to a symmetric bilinear expression involving the two pseudoscalar K's which consequently cannot be in a state with $J = 1$. The value of Θ_s deduced in this way is less accurate than that obtained from the mass formula but is consistent with it.

The measurement of the mixing angle using the e^+e^- decays of ω and φ depends upon the fact that the SU_3 singlet ω_0 is not coupled to the electromagnetic field. If this is true, the mixing angle Θ_s, is in fact obtained by measuring the ratio

$$R = \frac{\varphi \to e\bar{e}}{\omega \to e\bar{e}} \propto \cot^2 \Theta_{EM} .$$

(The suffix EM indicates that the mixing angle Θ_s is measured using electromagnetic channels instead of strong channels.)

There are two possible reasons why the mixing angle, Θ_{EM}, measured "electromagnetically" could differ from Θ_s:

a) The possible existence of the "charm" quantum number. If this quantum number were to exist, the Gell-Mann - Nishijima relation would contain another additive term and consequently the electromagnetic current would be

$$J_{em} \sim J_3 + \frac{J_8}{\sqrt{3}} + \frac{c}{3} \qquad \text{and not}$$

$$J_{em} \sim J_3 + \frac{J_8}{\sqrt{3}} \qquad \text{as has been believed so far.}$$

The electromagnetic field would then be able to couple to the singlet ω_0 and therefore give

$$\frac{\varphi \to e^+e^-}{\omega \to e^+e^-} \propto \cot^2 \Theta_{EM} = \left| \frac{\cos \Theta_s + X \sin \Theta_s}{- \sin \Theta_s + X \cos \Theta_s} \right|^2 \neq \cot^2 \Theta_s .$$

Notice that if $X = 0$, i.e. if the "charm" quantum number is not associated with the ω_0 then

$$\cot^2 \Theta_{EM} = \cot^2 \Theta_s ,$$

and we expect to find $\Theta_{em} \approx 38^\circ$.

b) The possible existence of the "A" quantum number. Brouzan and Low have proposed the existence of a special selection rule for bosons which originated the conserved "A" quantum number. If this selection rule is valid then

$\omega \to \gamma$ transitions are forbidden

while

$\varphi \to \gamma$ transitions are allowed.

The suppression generated by the "A" quantum number is believed to be a factor ~ 40, therefore we would expect $\Theta_{EM} \simeq 0^{\circ}$. Concerning the validity of this "A" quantum number no clear-cut experimental evidence exists at present. For instance, the η decays can be explained according to Okubo, without any need for the "A" quantum number conservation, by actually working out the detailed matrix elements for each channel. This, on the other hand, necessarily involves model-calculations. Nevertheless, the fact that by using a reasonable model it is possible to explain factors as large as 100 between expected* and observed rates casts much doubt on the existence of the "A" quantum number. Recently the missing decay mode ($\lesssim 3\%$) to $\eta\pi$ of the A_2 meson was shown by Glashaw and Socolow to be consistent with their expectations without any "A" conservation.

It is clear that if we measure $\Theta_{EM} \approx 38^{\circ}$ the "A" quantum number has to be disregarded.

iv) The comparison of the "electron" and the "muon" channels allows a check of the equality of the electromagnetic coupling of "μ" and "e" for a range of time-like q^2 from 0.56 $(\mathrm{GeV/c})^2$ to 1.44 $(\mathrm{GeV/c})^2$.** In this connection it is interesting to point out that a repetition of the large angle e^+e^- photoproduction experiment by Mistry et al., seems to confirm the results previously obtained by Pipkin et al. (Private communication from J. Steinberger). This result implies the existence of a "non-locality" associated with the "electron" which is as large as $(0.4\ \mathrm{GeV/c})^2$.

---

* Expected on the basis of phase space and the presence of γ-rays in the final state.

**In fact the production of (e^+e^-) and $(\mu^+\mu^-)$ pairs with large time-like q^2 values should be identical over all the range of q^2 values obtainable with present π, N beams. See also Appendix III.

2. THE PRESENT STATUS OF THE PRODUCTION OF VECTOR MESONS AND THEIR LEPTONIC DECAYS

We will briefly review what is known so far in this field. Table 1 shows the theoretically expected branching ratios of the φ, ω and ρ mesons, the present experimental results, and finally the expected rates for the present proposal.

The following points concerning the decays are to be noted:

i) The "electron" decay of the ρ is practically unknown, while the "muon" decay seems in good shape.

ii) The electron decay of the ω is poorly known. Notice, moreover, that the theoretical estimates reported in Table 1 do not take into account the possible depression factor due to the "A" or "Low" quantum number. As pointed out before, this could lead to a depression by a factor of 40 relative to the expected branching ratio.

iii) Nothing is known concerning the φ.

This lack of knowledge is not an accident but a serious consequence of the way in which φ's are produced in nature. In fact the expected leptonic branching ratio of the φ is an order of magnitude higher than that of the ω or ρ.

2.1 Production of ρ, ω and φ

Here it should be noticed that until now *) nobody had observed the production of φ's in pion-nucleon interactions. The φ's are known to be produced by K^-, and the upper limit for $\pi^+ p \to \varphi N^*$ is 10 μbarns at 3.65 GeV/c pion momentum.

---

*) After writing the present proposal we have received a communication that φ production has been observed in the reaction $\pi^- p \to \varphi N$ with $\sigma_\varphi/\sigma_\omega \simeq 10^{-2}$ for a pion momentum ranging from 1.57 to 2.22 GeV/c. Notice that this value is in good agreement with our value assumed in Table 1.

66/197/3
p/jmf

Another limit is

$$\frac{\pi^- p \to \pi^- p\, \varphi}{\pi^- p \to \pi^- p\, \omega} = 1.2\% \quad \text{at} \quad P_\pi = 3.7 \text{ GeV/c}$$

Figure 1 shows the variation of $\sigma_{\pi p \to n\omega}$ versus P_π, and in Fig. 2 the cross-section for ρ production is shown.

From the above discussion it follows that the first step must be the study of the production of φ in π-N interactions in order to establish definitely the feasibility of that part of the experiment concerned with the measurement of the (ω-φ) mixing angle. The method is discussed in Appendix II.

3. THE PROPOSED SET-UP

The principle of the experiment is as follows:

The ρ, ω and φ will be produced in the reaction

$$\pi^- + p \to \left\{ \begin{matrix} \rho \\ \omega \\ \varphi \end{matrix} \right\} + N$$
$$\hookrightarrow e^+ e^-$$

so the particles in the final state will be e^+, e^- and neutron. (We have also studied the possibility of looking at φ's produced in the reaction $K^- + p \to \varphi^0 \Lambda^0$ but this does not look very encouraging.)

3.1 The neutron detector

Figure 3 shows the neutron time-of-flight as a function of the neutron laboratory angle for various missing mass values at 3.0 GeV/c incident pion momentum. As may be seen from the curves a displacement of the neutron counter by $\sim 11^\circ$ is sufficient to vary the mass selection from φ to ω. The angular acceptance of the neutron counter in the φ position will be from 38° to 48°.

One possible type of neutron counter which we would like to use is a six-layer scintillator structure viewed by two photomultipliers which determine the azimuthal angle and by twelve photomultipliers which determine the polar angle and the time-of-flight using the Charpak-Dick-Feuvrais technique. The dimensions of the detector will be 60 cm × 40 cm × 30 cm.

The resolution in mass of this neutron detector is a result of time-of-flight and position resolutions. The latter is also a time resolution since we use the CDF technique. We are aiming at a time-of-flight resolution of 0.3 nsec which corresponds to $\Delta m = 7$ MeV. The spacial resolution aimed at is ± 2.5 cm over a distance of 2 metres, i.e. $\Delta\theta = \pm 0.7^{\circ}$ which corresponds to $\Delta m = 10$ MeV. The total mass resolution is therefore

$$\Delta m = \pm 12 \text{ MeV}$$

Total acceptance: $\left.\begin{array}{l}0.3 \text{ polar}\\ 0.5 \text{ azimuth}\end{array}\right\}$ 0.15 total angular acceptance.

Efficiency (averaged over the range 100 to 400 MeV kinetic energy)

= 30% .

Fraction of neutrons detected

= efficiency × acceptance = 4.5%.

3.2 The electron detector

Considerable experience has been gained during our previous experiment ($p\bar{p} \to e\bar{e}$) in the selection of electrons in the presence of a high pion background. Particularly simple criteria may be used to attain a rejection power of 5×10^{-4} in the energy interval 1.0 to 2.5 GeV. These detectors have been fully described in a published paper and will not be described further here.

66/197/3
p/jmf

For the above neutron acceptance the φ momenta and angles lie between 2.8 GeV/c at 3° and 2.2 GeV/c at 21°, which gives us the excellent possibility of triggering on the condition that the total amount of electromagnetic energy must be greater than 2.2 GeV. For the mean φ momentum, the minimum opening angle of the electrons is 45° and the distribution in opening angle is such that 75% of the events will have opening angles between 45° and 60°.

It is intended to add to our PAPEP detectors two gas Čerenkov counters between the first and second direction-defining chambers in order to give further rejection and reduction in trigger rate.

The mean acceptance of the electron detector is 30%, and by increasing the thickness so as to improve the energy resolution we expect to obtain high efficiency.

We have considered the possibility of a magnetic analysis of the electron pairs but at present this complication does not seem to be necessary.

3.3 Experimental layout

Figure 4 shows the side view of the experimental set-up. The target is 30 cm of liquid hydrogen. The electron directions are defined by thin-plate spark chambers placed 40 cm apart in front of the electron detectors. The neutron detectors are mounted at a mean angle of 43° at a distance of 2 metres from the target. They are six in number and span 50% of the neutron azimuth (see Fig. 5). Appendix I discusses the choice of neutron counter geometry.

Pulse-height analysis is carried out in the counters M to ensure that one and only one particle enters each electron detector. A 20 cm diameter beam veto counter is placed immediately before the electron detectors to veto non-interacting beam particles and some of the unwanted interactions. An annular veto counter shields the electron detector from the halo of the beam. Not shown on the diagram is a set of crossed hodoscope counters to select events with fixed opening angle, the veto counters which are placed in front of the neutron counters, and the hodoscope of beam counters which determine accurately the incident particle momentum.

4. EXPECTED RATE AND BACKGROUND

$$\text{Rate} = N_{\pi} \times N^{A} \times \rho \times \ell \times \sigma \times R \times \epsilon_n \times \epsilon_e$$

$$= 10^7 \times 6 \times 10^{23} \times 7 \times 10^{-2} \times 30 \times 3 \times 10^{-27} \times 10^{-4} \times 4.5 \times 10^{-2} \times 0.3$$

where

N_{π} = maximum beam rate = 10^7 π/burst (10^{12} circulating protons)

σ = production cross-section = 3 mbarns

R = branching ratio = 10^{-4}

$\rho\ell$ is the surface density of hydrogen

ϵ_n and ϵ_e are neutron and electron total acceptances.

This gives a rate of 2200 events/day with maximum beam, 10^{-4} branching ratio and 3 mbarns cross-section.

In the final column of Table 1, rates are quoted with the more realistic figures of 5×10^{11} protons/burst and 30% of these on target 1. Further, they are calculated using the theoretical branching ratios and reasonable production cross-sections.

4.1 Trigger rate from spurious events.

The electron detectors give a trigger from a π or K pair with $(5 \times 10^{-2})^2$ without total energy discrimination. From experience with similar conditions in the PAPEP experiment, we expect a further factor of 10 from the total energy discrimination. We estimate a factor of 10 for the combined effects of the beam veto counter, the single particle selecting counters, the gas Čerenkov counters and the kinematic selection. It will be seen that even without this extra factor the rate is reasonable.

66/197/3
p/jmf

The neutron trigger will restrict the missing mass to values around the resonance for which we are looking. It is therefore expected that the main trigger will come from the strong two-body decays of the resonances. The spurious trigger rate will then be:

(kinematic) × (electron detector)^2(total E.M. energy) × R^{-1}× event rate =

$$10^{-1} \times 2.5\times10^{-3} \times10^{-1} \times10^{4} \times 7.6\times10^{-6}$$

$$\approx 2\times10^{-3} \text{ triggers/burst}$$

$$= 1 \text{ trigger/20 minutes} .$$

4.2 Background rate in the chambers

Take total πp cross-section = 20 mbarns.

Number of interactions/burst = 3.8×10^{4}.

Pion multiplicity × duty cycle = 10 (say), so we will have a total rate 3.5×10^{5} particles/sec in each chamber. For a given good event, the probability that another interaction will take place during the sensitive time of the chamber ($\sim 10^{-6}$ sec) is 10^{-1}. It is intended to overcome this by displaying the first few electron detector counters on a slow oscilloscope so as to recognise when double events occur. In this way we expect to lose less than 5% of the events because of ambiguous double events.

5. REQUEST FOR MACHINE TIME AND BEAM REQUIREMENTS

Six weeks are requested for setting up and measuring the production of φ, ω and ρ.

The request for run-time will be made after these tests.

The beam requirements are 30% to 40% on target 1, at 19.2 GeV internal beam momentum and 300 msec flat-top. The external beam required is $m_{4\alpha}$ with beam momentum variable up to 3.0 GeV/c.

66/197/3
p/jmf

Appendix I

Angular distributions and polarisation states of the vector mesons

The cylindrical symmetry of our neutron detector is designed in order to produce a zero mean polarization of the vector mesons. This is important for a comparison of the φ and ω branching ratios because they may be produced with different polarization.

The variation of the neutron counting rate with the neutron azimuth will allow a measurement of the product αP

α = parameter of the angular distribution

P = polarization of the vector meson

where

$$\frac{dN}{d\Omega} \sim 1 + \alpha \cos^2 \Theta$$

$$\alpha = \frac{3|A+|^2 + 3|A-|^2 - 1}{1 - |A+|^2 - |A-|^2}$$

where $A\pm$ are the helicity ± 1 amplitudes.

Figure 6 shows possible decay distributions for $\alpha = \pm 1$.

66/197/3
p/jmf

Appendix II

Search for φ production in pion-nucleon interactions

It is intended that this search will also be a test of the performance of the prototype neutron counter and so this is used as described in the main text.

The φ's will be detected using the decay mode K^+K^- and use will be made of the low Q-value of this decay. Figure 7 shows the K opening angle distribution for φ energies corresponding to the range spanned by the neutron counters. Seventy per cent of the decays have the opening angle within 3^o of the maximum value.

The main background in this distribution comes from three pion events with invariant mass near to that of the φ mass. In order to estimate this effect, the decay $\varphi \to \pi^+\pi^-\pi^o$ at 2.5 GeV/c was simulated by Monte Carlo. One hundred and seventeen decays were used and the shaded squares show the tail of this distribution.

Thus, about 2% of the three-pion events are able to simulate $\varphi \to K^+K^-$. It is kinematically impossible for two-pions with invariant mass near that of the φ to simulate the φ decay. The problem of identifying the φs is then by this technique very similar to that of identifying φ's in normal missing mass spectrometry.

In order to be sure of selecting K^+K^- pairs, a K^+ detector will be used.

66/197/3
p/jmf

Appendix III

Two photon diagrams and related speculations

Throughout this paper we have neglected two-photon diagrams such as DIAG C on the basis that, for these types of diagrams, no

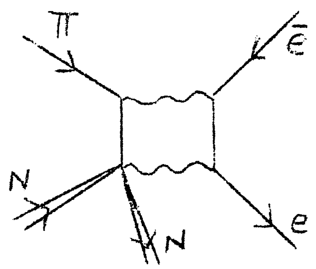

(DIAG C)

enhancement mechanism is known so far that will overcome the factor of $\alpha \sim 10^{-2}$ which they possess relative to DIAG A because of the second gamma ray. The interference term with the one-photon diagram vanishes for our present experimental conditions of observation.

This is equivalent to saying that the observation of an (e^+e^-) pair is considered as the signature that a time-like photon has been produced, i.e. a "hadron" with quantum numbers $J^{PC} = 1^{--}$, and I = 0, 1 ($G = \pm 1$) has transformed itself into a time-like photon. All the "unphysical region" can be scanned to look for such states; this scanning corresponds in fact to a complete investigation of the spectral functions entering in the dispersion integrals of the nucleon form factors. If this spectral function were found to be not very small outside the φ, ρ, ω peaks (i.e. little or no pole dominance), then we would propose to investigate the $\bar{\mu}\mu$ channel in order to compare ee and $\mu\mu$ results. In this comparison, all complications from strong interaction physics disappears and we remain with a clean investigation of the electromagnetic equivalence between "e" and "μ" for a large range of time-like q^2.

If the rates for lepton pairs produced in (πN) interactions turn out to be encouraging, the study of the interference term between one-photon and two-photon diagrams can be undertaken by distinguishing the sign of the charge of the leptons. If the interference term is not small this is a way of:

66/197/3
p/jmf

i) studying the q^2 dependence of the two-photon contribution in the nucleon form factors and

ii) by comparing $\bar{e}e$ and $\bar{\mu}\mu$ channels to investigate the point-like behaviour of "μ" and "e" propogators. In fact, when we limit ourselves to one-photon diagrams we only check electron and muon vertex functions. As is well known, vertex and propogator are related by the Ward Identity. Present evidence could be interpreted as indicating that there is a possible deviation from point-like behaviour for the electron propogator and probably no deviation for the electron vertex. It is not impossible that a breakdown of the point-like interaction between lepton and electromagnetic field would also violate the Ward Identity leaving the deviation from point-like behaviour entirely in the propogator.

References

Particular references will be supplied on request.

66/197/3
p/jmf

Figure Captions

1. Showing the cross-section for the production of ω in the reaction $\pi^- + P \rightarrow \omega + N$ as a function of the laboratory momentum of the pion.

2. Showing the cross-section for the production of ρ in the reaction $\pi^- + P \rightarrow \rho + N$ as a function of the laboratory momentum of the pion.

3. Showing the relationship between the neutron time-of-flight and the neutron laboratory angle for various values of the missing mass X in the reaction $\pi^- + p \rightarrow X^0 + N$ at 3.0 GeV/c incident pion momentum. The ordinate is the time-of-flight/metre - 3.33 nsec/m. The missing mass values used were

$$\varphi = 1020 \text{ MeV}, \ \eta_{\pi\pi} = 960 \text{ MeV}, \ \omega = 783 \text{ MeV}, \ \eta = 549 \text{ MeV}.$$

The range of, for example, the φ curve which is accepted by our set-up is 38^0 to 48^0 indicated by the "boxes".

4. Side view of the set-up. The beam crosses a hodoscope (not shown) which defines its momentum, passes through a veto counter to remove "Halo" and enters a 30 cm long hydrogen target. Thin plate spark chambers define the electron directions, and scintillation counters are used to select only events in which one particle enters each electron detector. A veto counter, immediately before the electron detector vetoes events at less than 12^0 and the electron detectors are similar to the ones used in the PAPLEP experiment. A hodoscope to recognise events within a fixed range of opening angle will be placed between the thin plate spark chambers and the electron detector. The neutron counter consists of six layers of scintillator viewed collectively by two photomultipliers in the azimuthal direction and by twelve photomultipliers in the polar direction. The veto counters in front of the neutron counters are not shown.

5. Showing the end view of the set-up.

66/197/5
p/jmf

6. Showing the extreme types of angular distribution of the decay electrons in the laboratory system. The vector meson is produced with a polarisation perpendicular to the production plane (top diagram). The two extreme angular distributions are $\sin^2\Theta$ and $\cos^2\Theta$ where Θ is the angle between the vector meson spin direction and the decay electron direction. These are sketched, distorted by the Lorentz transformation, in the left and right lower parts of the diagram, and show how the vector meson spin should be orientated relative to the two electron detectors in order to have the maximum detection efficiency.

7. Showing the opening angle distribution for $\varphi \to K^+K^-$ for φ momenta of 2.0, 2.5 and 3.0 GeV/c. The line marked 70% indicates the region containing this fraction of the decays for the 2.5 GeV/c curve. The shaded squares indicate the background expected in this region of opening angle from final states of the reaction $\pi^- + p \to n + 3\pi$ at 2.5 GeV/c. Roughly, the smallest square represents 1% background.

66/197/3
p/jmf

TABLE I

Theoretical	Experimental	Expected
$\frac{\Gamma_{\rho \to \bar{e}e}}{\Gamma_\rho} \approx (5.7 \pm 0.3) \times 10^{-5}$ *)	$\frac{\Gamma_{\rho \to \bar{e}e}}{\Gamma_\rho} = \left(5^{+6}_{-3}\right) \times 10^{-5}$ (Madanski et al.) $\frac{\Gamma_{\rho \to \bar{\mu}\mu}}{\Gamma_\rho} = \left(3.3^{+1.6}_{-0.7}\right) \times 10^{-5}$ (Weinstein et al.) 1000 $\rho \to \mu\mu$ observed by Wilson et al.	68 events/day for $\sigma_\rho = 1$ mbarn production cross-section.
$\frac{\Gamma_{\omega \to \bar{e}e}}{\Gamma_\omega} \approx (7.4 \pm 0.1) \times 10^{-5}$ *)	$\frac{\Gamma_{\omega \to \bar{e}e}}{\Gamma_\omega} = \left(10^{+12}_{-8}\right) \times 10^{-5}$ (Madanski et al.) $\frac{\Gamma_{\omega \to \bar{e}e}}{\Gamma_\omega} = (60 \div 5) \times 10^{-5}$ (Newth et al.)	250 events/day for $\sigma_\omega = 3$ mbarn. This may be 6 events/day if the Low quantum number is operative: $\sim (40)^{-1}$ depression factor.
$\frac{\Gamma_{\varphi \to \bar{e}e}}{\Gamma_\varphi} \approx (55 \pm 10) \times 10^{-5}$ *)		19 events/day for $\sigma_\varphi = 10^{-2}\ \sigma_\omega$. No depression factor expected

*) The errors quoted reflect only the uncertainty in the measured total width of the resonance.
It should be emphasized that the theoretical uncertainties indicated by the sign ≈ are indeed much larger.

Fig. 1

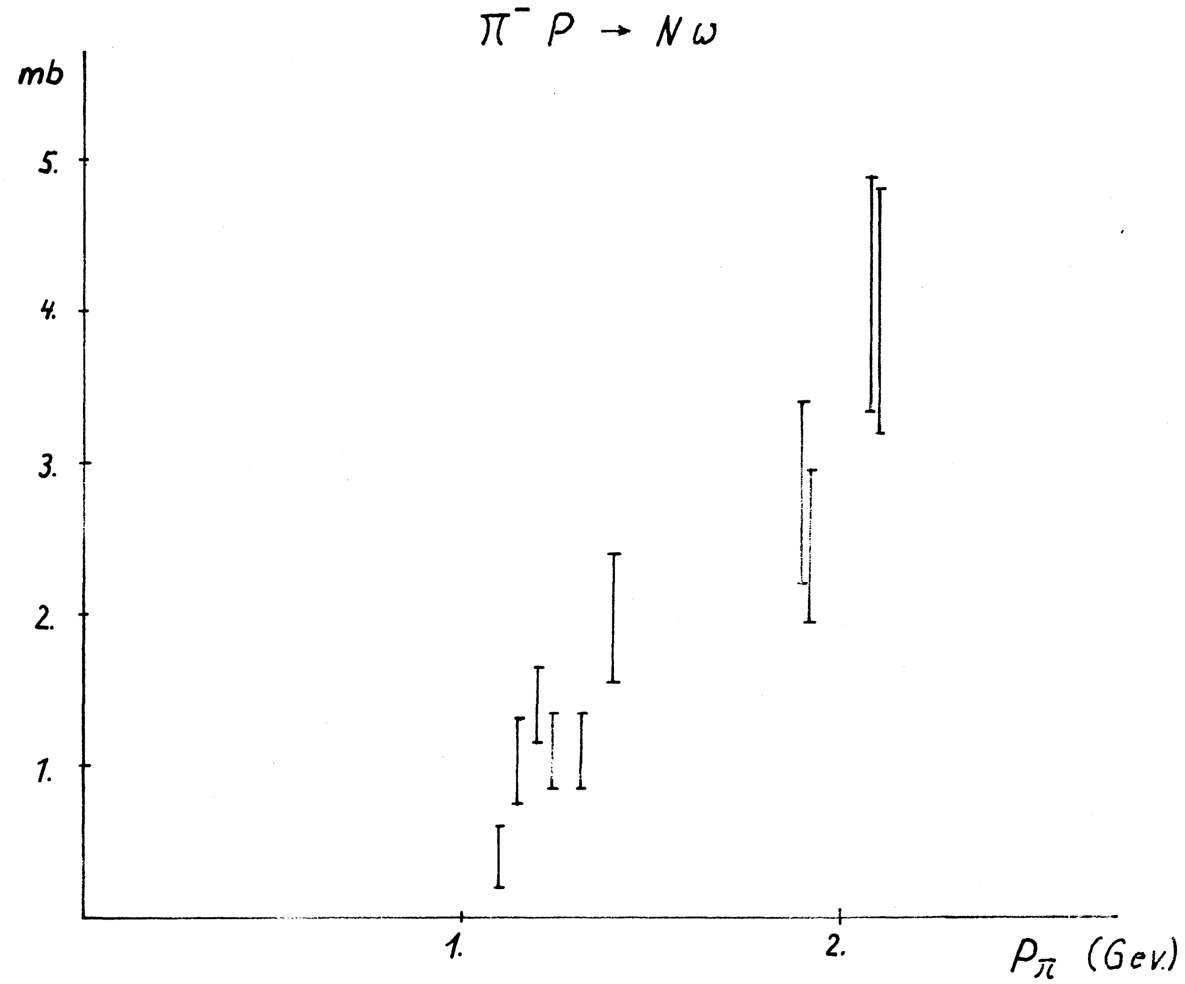
$\pi^- p \to N\omega$
mb
5.
4.
3.
2.
1.
1.
2.
p_π (Gev.)

Fig. 2

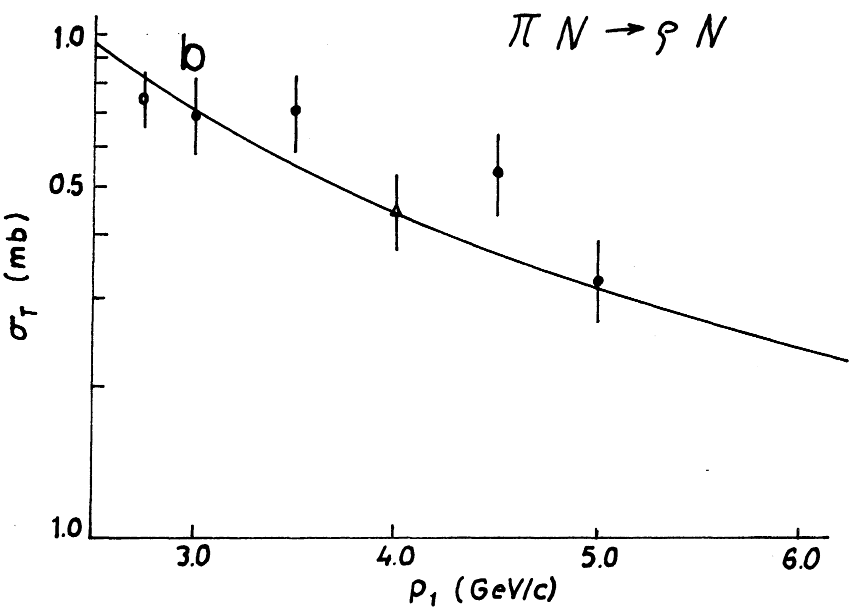
$\pi N \to \rho N$
b
1.0
0.5
1.0
σ_T (mb)
3.0
4.0
5.0
6.0
p_1 (GeV/c)

FIG. 3

Neutron time of flight spectra in $\pi^- + p \to N + X$ at 3.0 Gev/c

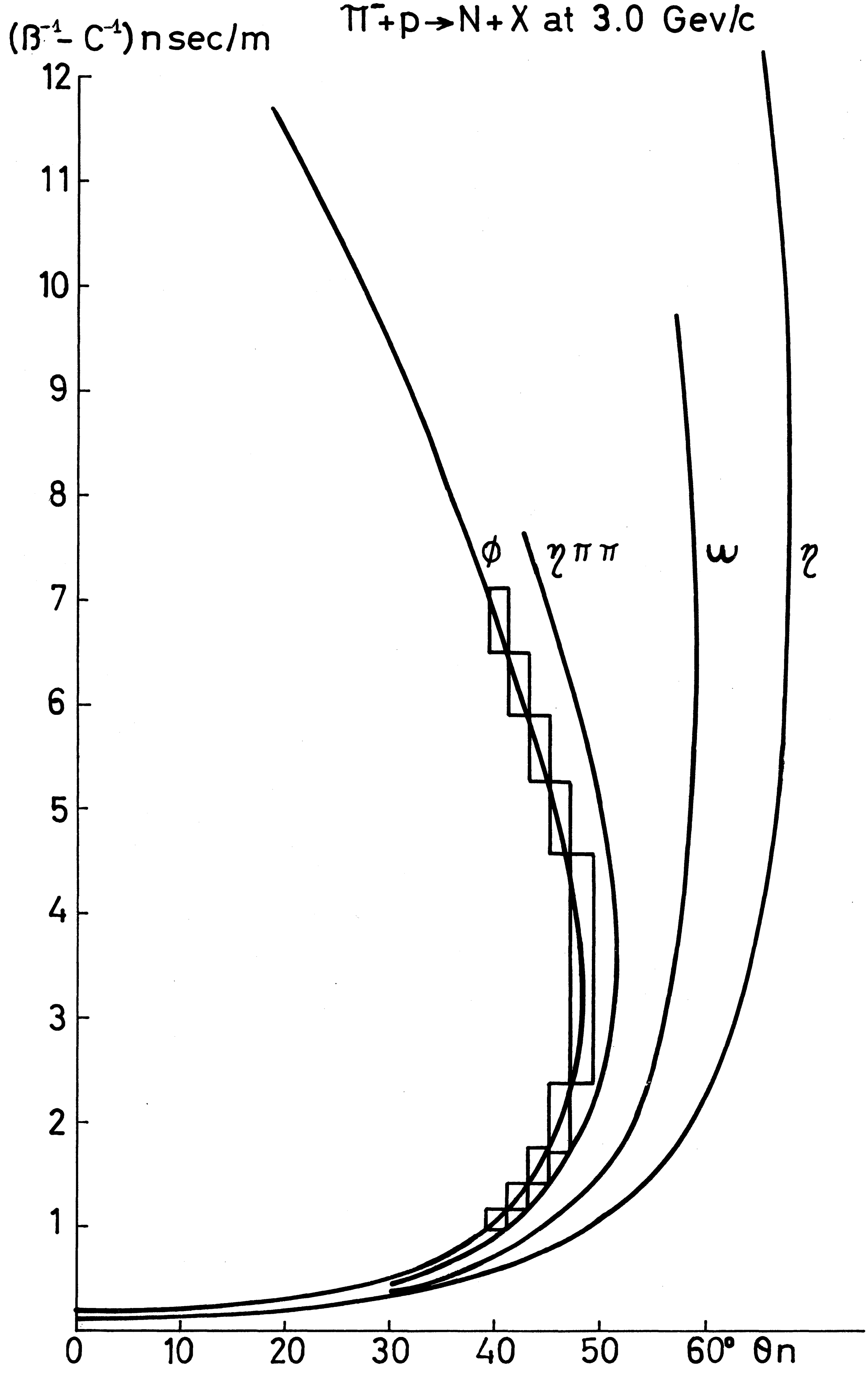

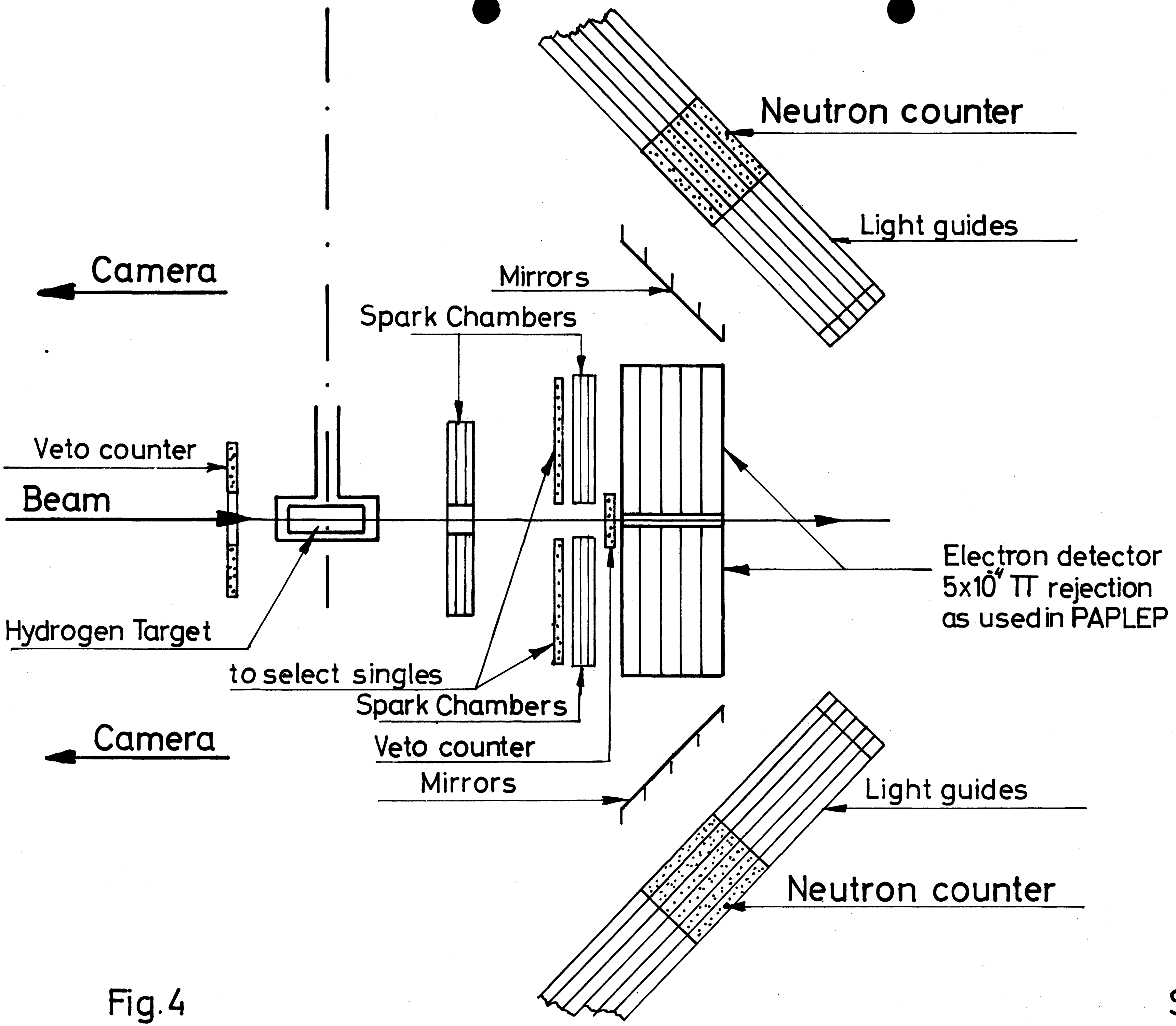

Fig. 4

Scale 1/20

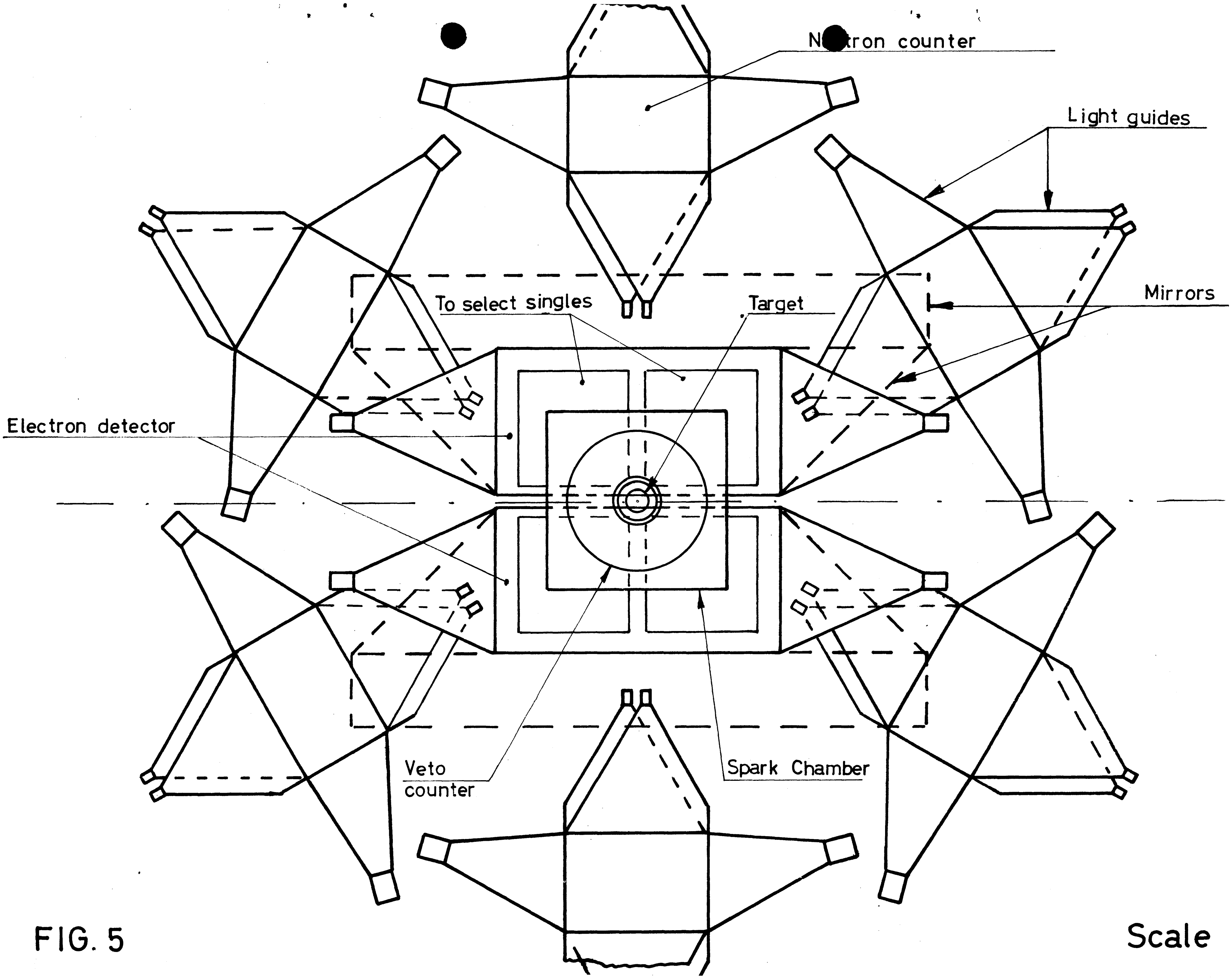

FIG. 5

Scale 1/20

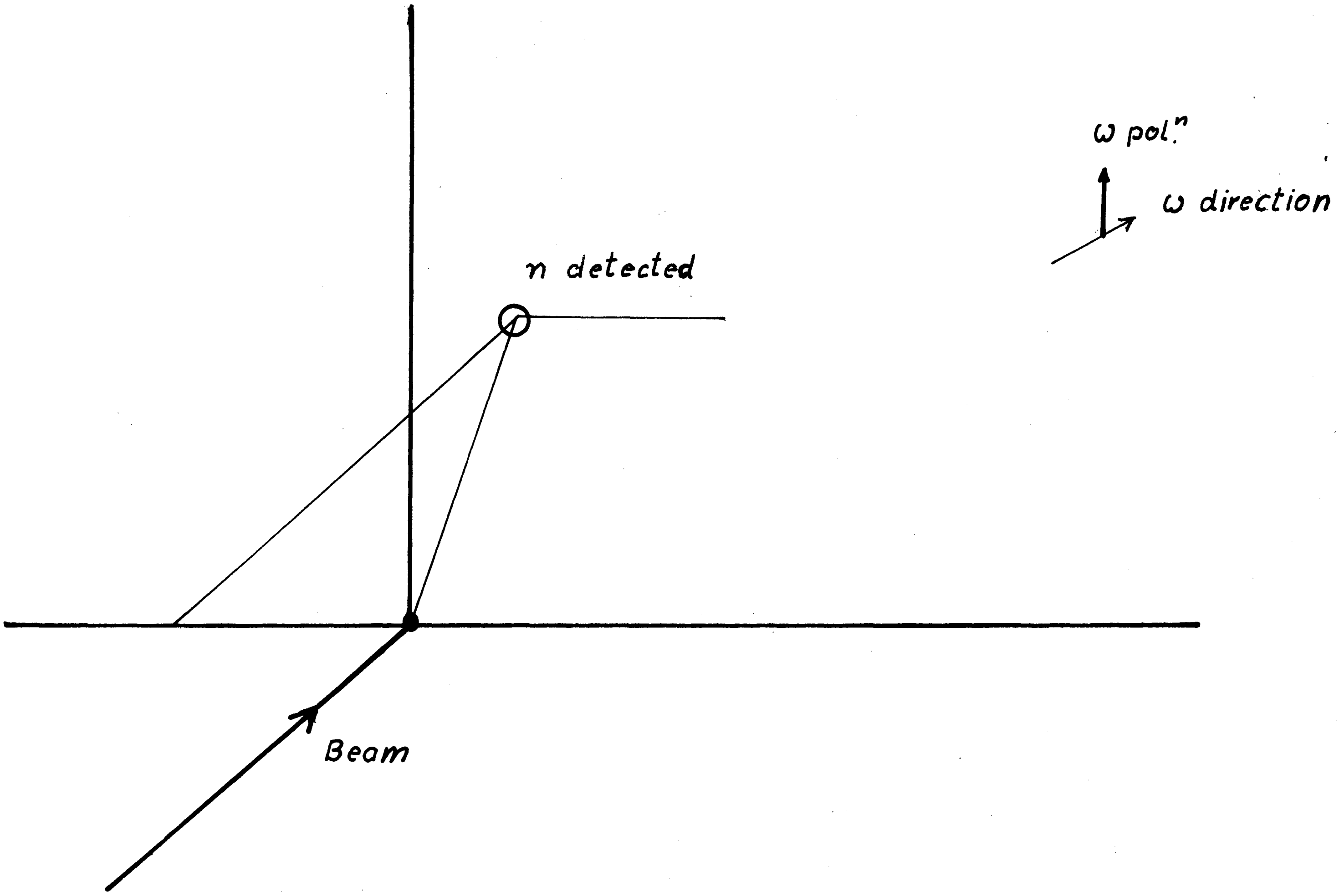

Fig. 6

$|A| = 0$, $\sin^2\theta$ decaydist.^{n} is

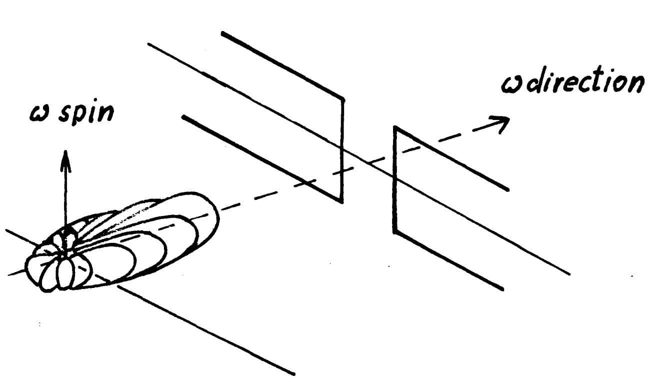

$|A| = 1$, $\cos^2\theta$ decaydist.^{n} is

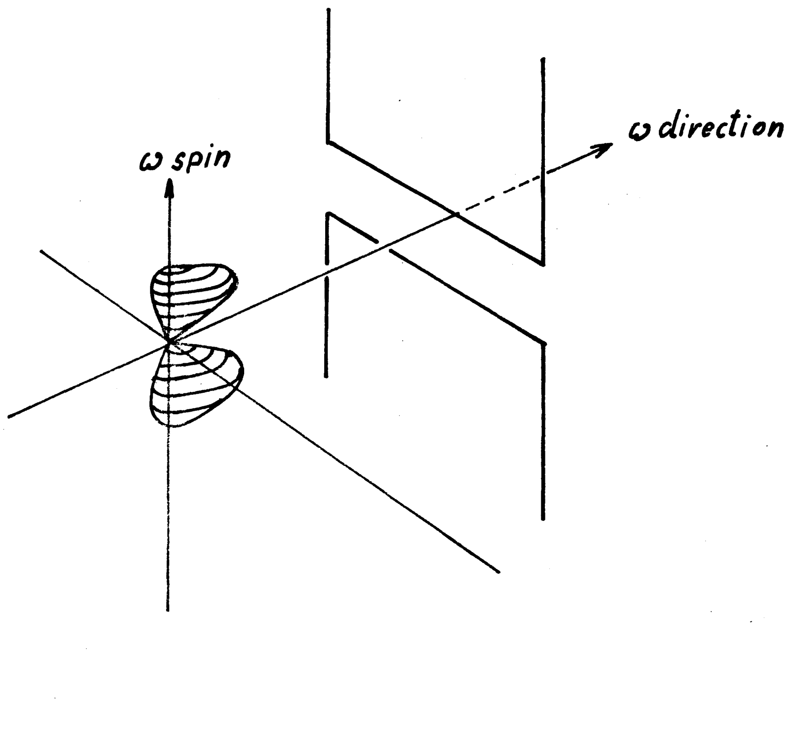

Fig. 7 Opening angle distribution for $\phi \rightarrow k^+ k^-$